NEOPLASIA
www.neoplasia.com

Volume 10 Number 4 April 2008 pp. 303–313 303

Noninvasive Magnetic Resonance Spectroscopic Pharmacodynamic Markers of a Novel Histone Deacetylase Inhibitor, LAQ824, in Human Colon Carcinoma Cells and Xenografts[1]

Yuen-Li Chung*, Helen Troy*, Rebecca Kristeleit†, Wynne Aherne†, L. Elizabeth Jackson‡, Peter Atadja§, John R. Griffiths*,2, Ian R. Judson†, Paul Workman†, Martin O. Leach‡ and Mounia Beloueche-Babari‡

*Cancer Research UK Biomedical Magnetic Resonance Research Group, Department of Basic Medical Sciences, St. George's University of London, London, UK; †Cancer Research UK Centre for Cancer Therapeutics, Haddow Laboratories, The Institute of Cancer Research, Sutton, Surrey, UK; ‡Cancer Research UK Clinical Magnetic Resonance Research Group, The Institute of Cancer Research and Royal Marsden Hospital, Sutton, Surrey, UK; §Novartis Institutes for Biomedical Research, Cambridge, MA, USA

Abstract

The aim of this work was to use phosphorus magnetic resonance spectroscopy (^{31}P MRS) to investigate the pharmacodynamic effects of LAQ824, a histone deacetylase (HDAC) inhibitor. Human HT29 colon carcinoma cells were examined by ^{31}P MRS after treatment with LAQ824 and another HDAC inhibitor, suberoylanilide hydroxamic acid. HT29 xenografts and tumor extracts were also examined using ^{31}P MRS, pre– and post–LAQ824 treatment. Histone H3 acetylation was determined using Western blot analysis, and tumor microvessel density by immunohistochemical staining of CD31. Phosphocholine showed a significant increase in HT29 cells after treatment with LAQ824 and suberoylanilide hydroxamic acid. *In vivo*, the ratio of phosphomonoester/total phosphorus (TotP) signal was significantly increased in LAQ824-treated HT29 xenografts, and this ratio was inversely correlated with changes in tumor volume. Statistically significant decreases in intracellular pH, β-nucleoside triphosphate (β-NTP)/TotP, and β-NTP/inorganic phosphate (Pi) and an increase in Pi/TotP were also seen in LAQ824-treated tumors. Tumor extracts showed many significant metabolic changes after LAQ824 treatment, in parallel with increased histone acetylation and decreased microvessel density. Treatment with LAQ824 resulted in altered phospholipid metabolism and compromised tumor bioenergetics. The phosphocholine and phosphomonoester increases may have the potential to act as pharmacodynamic markers for noninvasively monitoring tumor response after treatment with LAQ824 or other HDAC inhibitors.

Neoplasia (2008) 10, 303–313

Abbreviations: ^{1}H MRS, proton magnetic resonance spectroscopy; ^{31}P MRS, phosphorus magnetic resonance spectroscopy; DMSO, dimethylsulfoxide; FCS, fetal calf serum; GPC, glycerophosphocholine; GPE, glycerophosphoethanolamine; HDAC, histone deacetylase; HIF-1α, hypoxia-inducible factor 1 alpha; Hsp70, heat shock protein 70; Hsp90, heat shock protein 90; i.p., intraperitoneally; NTP, nucleoside triphosphate; PC, phosphocholine; PCr, phosphocreatine; PDE, phosphodiester; PE, phosphoethanolamine; PME, phosphomonoester; Pi, inorganic phosphate; SAHA, suberoylanilide hydroxamic acid; TotP, total phosphorus; VEGF, vascular endothelial growth factor

Address all correspondence to: Dr. Yuen-Li Chung, Cancer Research UK Clinical Magnetic Resonance Research Group, The Institute of Cancer Research and Royal Marsden Hospital, Downs Road, Sutton, Surrey SM2 5PT, UK. E-mail: ylichung@icr.ac.uk

[1]Financial support: Cancer Research UK (grant nos. C12/A5096; C1060/A5096 for Y.-L. C., J. R. G. and H. T.; C1060/A6916 for M. B.-B.; C160/A808 for M. O. L. and L. E. J.; and C309/A2187; C309/A8274 for P. W., I. J., W. A., and R. K.). P. W. is a Cancer Research UK Life Fellow.

[2]Present address: Cancer Research UK Cambridge Research Institute, Cambridge, UK.

Received 12 December 2007; Revised 27 January 2008; Accepted 28 January 2008

DOI 10.1593/neo.07834

Introduction

DNA is packaged into chromatin in eukaryotic cells. The functional and structural properties of chromatin can be influenced by various posttranslation modifications of the amino-terminal tails of nucleosomal histones. Histone acetylation plays an important role in the regulation of transcription, replication, and DNA repair [1–3]. Acetylation is regulated by the opposing effects of two families of enzymes, histone acetyltransferases and histone deacetylases (HDACs). Histone acetyltransferases catalyze the addition of acetyl groups, whereas HDACs catalyze the reverse reaction. Previous studies have found evidence that aberrant recruitment of HDACs may cause specific changes in gene expression profiles in transformed cells [4–7]. Deregulation of histone acetylation has also been associated with the development of various human cancers [4–7].

Inhibition of HDAC causes modification of chromatin structure and results in activation (e.g., p53, p21, and caspases) and deactivation [e.g., hypoxia-inducible factor 1 alpha (HIF-1α) and vascular endothelial growth factor (VEGF)] of a variety of genes that mediate proliferation, cell cycle progression, angiogenesis, and apoptosis [7–19]. In addition to their effect on histones, certain HDAC inhibitors also interact directly with various proteins whose function is modified by acetylation. These include some transcription factors (e.g., E2F-1 and NF-κB), several signal transduction mediators (e.g., pRB), and the heat shock protein 90 (Hsp90), a molecular chaperone that maintains the stability and maturation of several oncoproteins, including C-RAF, AKT, and ErbB2 [19–24]. Thus, inhibition of HDAC is expected to impact on the activation of several oncogenic and survival-related pathways.

The HDAC inhibitor, LAQ824, is effective against several human tumor models [13,22–26]. LAQ824 inhibits VEGF-induced angiogenesis, causes cell cycle arrest, and induces apoptosis in human cancer cells and xenograft models [13,22–26].

The rational development of new molecular cancer therapeutics requires the discovery and validation of biomarkers of drug action [27–29]. These are valuable because they can provide proof of concept for the intended mechanism of action in phase I clinical studies and aid in dose selection for phase II trials. A recent study has shown that, in the majority of phase I trial designs for the investigation of targeted, noncytotoxic agents in solid tumors, traditional endpoints rather than molecular measures of drug effects are used for the selection of the recommended phase II dose [30]. This is probably due, in most cases, to the difficulty of obtaining the tumor biopsies that are required to perform standard assays of drug action on molecular targets. The development of surgically noninvasive endpoints is, therefore, particularly important because they would avoid the need for tumor biopsy [27].

In vivo phosphorus magnetic resonance spectroscopy (^{31}P MRS) is a noninvasive technique that provides biochemical information about both healthy and diseased tissues in many parts of the body [31]. This technique has also been used to study the biochemistry and physiology of tumor cells and solid cancers, and it has shown potential in the assessment of response after therapies in both human and animal models [32–39]. Markers for tissue bioenergetics, such as nucleoside triphosphates (NTPs), inorganic phosphate (Pi), and intracellular pH (pHi), as well as various phosphorus-containing components of phospholipid metabolism, are readily observed using ^{31}P MRS. In tumors, the phosphomonoesters (PMEs) are mainly phosphocholine (PC) and phosphoethanolamine (PE), precursors of the membrane phospholipids phosphatidylcholine and phosphatidylethanolamine, respectively, whereas the phosphodiesters (PDEs) are glycerophosphocholine (GPC) and glycerophosphoethanolamine (GPE), which are breakdown products of phosphatidylcholine and phosphatidylethanolamine, respectively. Therefore, changes in phospholipids could provide useful information about tumor cell membrane metabolism. However, in several published studies, the changes in the phospholipid have been attributed to the modulation of various signaling pathways and were mostly independent of membrane metabolism [38,39].

To predict the efficacy of LAQ824 by ^{31}P MRS *in vivo* in clinical trial patients, we investigated the pharmacodynamic effects of LAQ824 in a human colon carcinoma model in mice, using both *in vitro* and *in vivo* MRS techniques, because MR spectra of biopsy extracts yields better peak resolution; ^{1}H MRS was used on tumor extracts *ex vivo* to characterize changes in nonphosphorylated metabolites. We also examined ^{31}P MR spectra of extracts of a human colon carcinoma cell line, HT29, using two different HDAC inhibitors: suberoylanilide hydroxamic acid (SAHA; Vorinostat) [40] and the novel HDAC inhibitor, LAQ824 [24]. Suberoylanilide hydroxamic acid was included in these experiments as a second HDAC inhibitor with a different chemical structure to verify that some of the effects seen with LAQ824 were associated with HDAC inhibition. We also conducted an *in vivo* MRS study on the effects of LAQ824 on the HT29 xenograft model: (1) to demonstrate therapeutic efficacy; (2) to determine whether MRS changes observed in the cell studies were reproducible *in vivo*; and (3) to investigate whether ^{31}P MRS could provide a noninvasive pharmacodynamic biomarker for the therapeutic action of HDAC inhibitors that could be used in future clinical trials. In addition, the effects of LAQ824 on tumor microvessel density and histone H3 acetylation status were determined to see if vascular and molecular effects accompanied changes in the MR spectrum. As HDAC inhibition impacts on Hsp90 activity [19–24], we also probed for the molecular signature of Hsp90 inhibition by determining levels of the client protein C-RAF and the molecular cochaperone heat shock protein 70 (Hsp70).

Materials and Methods

Materials

LAQ824 was provided by Novartis (Hanover, NJ) and SAHA was purchased from Alexis Corporation (Nottingham, UK). Both drugs were dissolved in dimethylsulfoxide (DMSO) and stock solutions were stored at −20°C. Dulbecco's modified Eagle's medium, fetal calf serum (FCS), penicillin, and streptomycin were purchased from Gibco (Paisley, UK); EDTA, perchloric acid (PCA), and potassium hydroxide were from Merck (Poole, UK); Hypnorm was obtained from Jansen Pharmaceuticals (Buckinghamshire, UK); Hypnovel was from Roche (Welwyn Garden City, UK); and all other chemicals were purchased from Sigma (Poole, UK).

Cell Culture

HT29 human colon carcinoma cells were grown in Dulbecco's modified Eagle's medium containing 10% heat-inactivated FCS with 100 U/ml penicillin and 100 μg/ml streptomycin. Cells were maintained at 37°C in a humidified 5% CO_2 atmosphere, and growth media were replenished every 48 hours.

Growth Inhibition Assay

The effect of drug treatment on cell proliferation was measured using the sulforhodamine B (SRB) assay [41]. For this, cells growing

in 96-well microtiter plates were treated with varying concentrations of LAQ824 or SAHA for 96 hours. At the end of incubation, plates were fixed in 150 μl of cold trichloroacetic acid for 30 minutes then stained overnight with 0.4% (w/v) SRB made up in 1% acetic acid. Plates were washed in 1% acetic acid to remove excess dye, treated with 150 μl of 10 mM Tris to dissolve protein-bound SRB and then read on a plate reader at 570 nm (Molecular Devices, Sunnyvale, CA).

HDAC Inhibition for In Vitro *MR Measurements*

HT29 cells were treated with 34 μM SAHA [i.e., 20× of the 50% growth inhibition concentration (GI_{50})] and 350 nM LAQ824 (i.e., 10× GI_{50}) for 24 hours to achieve a ca. 50% decrease in cell number per flask and an inhibition of HDAC as measured by Western blot analysis (see below) at the time of cell extraction. Higher concentrations of SAHA and LAQ824 were used to treat HT29 cells because the GI_{50} values quoted previously were based on 96 hours' drug exposure rather than the 24 hours' exposure used in these experiments. The effect of HDAC inhibition on cell counts was assessed by determining the number of attached cells using the trypan blue exclusion method.

HT29 Tumor Xenograft Model

Eight-week-old MF-1 male nude mice, weighing 30 to 38 g, were injected subcutaneously in the flank with 0.2 ml of HT29 (2.5×10^7 cells/ml) human colon carcinoma cells that had been grown as a monolayer in culture [36]. Tumor volume was calculated by measuring the length, width, and depth of each tumor using calipers and by using the following formula: $l \times w \times d \times (\pi/6)$. Once an appropriate tumor size (approximate volume of 500 mm^3) was established, mice were randomly divided into two groups; one group was treated with LAQ824 in the delivery vehicle (10% of DMSO and 90% of 5% dextrose in water) at 25 mg/kg intraperitoneally (i.p.) once a day for 2 days (n = 20; initial tumor volume, 537 ± 31 mm^3) and one group was treated with the delivery vehicle alone (n = 18; initial tumor volume, 484 ± 36 mm^3). A cohort of animals (7 vehicle- and 11 LAQ824-treated) was used in the MRS study, and tumors were excised on day 4 for Western blot, histologic, vascular, or *in vitro* MRS analysis. Tumors from another cohort of animals (6 vehicle- and 4 LAQ824-treated) were excised on day 4 and were used for histologic or Western blot analysis. A third cohort of animals (5 vehicle- and 5 LAQ824-treated) was used in the tumor growth delay study where the animals were treated for 2 days (same dosing schedule as the MRS study), and the tumor volumes were monitored for a further 8 days after the last dose. Animals were treated in accordance with the local and national ethical requirements and with the United Kingdom Co-ordinating Committee on Cancer Research Guidelines for the Welfare of Animals in Experimental Neoplasia [42].

Despite that the mouse tumors have a higher tumor-to-host weight ratio than human tumors, the previously reported noninvasive MRS biomarkers have been useful in translating into clinic [32–34].

In Vitro *^{31}P MRS of Cell Extracts*

Control and treated cells were extracted in equal volumes of cold methanol, chloroform and water, and lyophilized samples of the water-soluble fraction were reconstituted in 700 μl of deuterated water (D_2O) containing 10 mM EDTA and 2 mM methylenediphosphonic acid (an internal reference) at pH 8.2 [43]. ^{31}P MR spectra were recorded on a 500-MHz spectrometer (Bruker, Coventry, UK) using power-gated composite-pulse ^{1}H decoupling, a 30° flip angle, a 2-second repetition time and a spectral width of 100 ppm. Data were processed using a line broadening of 1 Hz and were analysed using MestRe-C version 2.3 (University of Santiago de Compostela, Spain). The metabolite content was determined by peak integration, normalized relative to the internal standard, and corrected for saturation and cell number in each sample.

In Vivo *^{31}P MRS of HT29 Tumor Xenografts*

Animals were anesthetized with a single i.p. injection of a Hypnovel-Hypnorm-water (1:1:2) mixture as previously described [36]. Animals were placed in the bore of a 4.7-T nuclear magnetic resonance (NMR) spectrometer (Varian, Palo Alto, CA) at St. George's University of London, and tumors were positioned in the center of a 12-mm two-turn ^{1}H/^{31}P surface coil. Image-selected *in vivo* spectroscopy–localized ^{31}P MR spectra of the tumors were obtained at 37°C as previously described [44]. Briefly, a gradient strength of up to 7.5×10^{-4} T/cm was applied with adiabatic pulses of 800 milliseconds, a sin/cos 90° excitation pulse, and a sech 180° inversion pulse, with a total repetition time of 3 seconds and 600 averages. *In vivo* ^{31}P MRS of the tumors was carried out before treatment (i.e., day 1) and the day after the last dose (i.e., day 4). Proton decoupling was not used in these experiments because it was not available in our MR system. ^{31}P MR spectra were quantified using the Variable Projection program (VARPRO) to determine precise chemical shifts and peak integrals as previously described [45]. After the final ^{31}P MRS study, the tumors were excised, and part of the tumor was snap-frozen for immunohistochemical staining of CD31 and part was freeze-clamped and stored at −80°C for subsequent immunoblot analysis or extraction for *in vitro* ^{1}H and ^{31}P MRS analyses. The excised tumors were weighed after freezing to minimize tissue degradation.

The surface coils used to obtain the ^{31}P MRS signal from subcutaneous tumors *in vivo* are of a nonuniform spatial sensitivity, making it impossible to use an external standard. As a result, the signal intensities observed in the *in vivo* ^{31}P MR spectra are expressed as ratios of metabolites.

In Vitro *^{1}H and ^{31}P MRS of Tumor Extracts*

About 200 mg of the freeze-clamped HT29 tumors were extracted in 6% ice-cold PCA, and the extraction procedures were performed on ice as previously described [46]. Neutralized extracts were freeze-dried and reconstituted in 1 ml of D_2O, and the extracts (0.5 ml) were placed in 5-mm NMR tubes. For the ^{1}H MRS, the water resonance was suppressed by using gated irradiation centered on the water frequency. Sodium 3-trimethylsilyl-2,2,3,3-tetradeuteropropionate (50 μl, 5 mM) was added to the samples for chemical shift calibration and quantification. Immediately before the MRS analysis, the pH of the samples was readjusted to 7 with PCA or potassium hydroxide. For the ^{31}P MRS, which was carried out after the ^{1}H MRS study, EDTA (50 μl, 60 mM) was added to each sample to chelate metals ions, and MDPA (50 μl, 5 mM) was added to each sample for chemical shift calibration and quantification. The extract spectra for both the control and the treated animals were acquired under identical conditions.

In vitro MRS was performed on tumor extracts to confirm our *in vivo* MR findings. Water-soluble metabolites were measured *in vitro* to provide the most appropriate match to our *in vivo* results. The PCA extraction method was used, because this is the method that is routinely carried out on tumor samples in our laboratory. However, we have used a dual-phase extraction method (methanol and chloroform) on cell

extracts *in vitro* and detected similar changes in the water-soluble fractions as those detected in the PCA-extracted tumors.

Western Blot Analysis

The molecular effects of HDAC inhibition on HT29 cells and xenografts were assessed by Western blot analysis for levels of acetyl histone H3, C-RAF, and Hsp70 protein expression. Cell pellets were resuspended in lysis buffer A (150 mM NaCl, 28.2 mM Tris-HCl, 1.1 mM Tris base, 0.2% sodium dodecyl sulfate, 1% Nonidet P-40, 10% glycerol, 0.5 mM sodium orthovanadate, 10 mM sodium pyrophosphate, 0.1 M NaF, and 1 mM EDTA) and 50 to 100 mg of ground tumor tissues were resuspended in lysis buffer B (150 mM NaCl, 50 mM Tris, pH 7.4, 1 mM EDTA, 1% Triton X-100, 1 mM NaF, 1 mM sodium orthovanadate, 1% protease cocktail, 1 mM dithiothreitol, 0.1% fenvalerate, and 1 mM phenylmethylsulfonyl fluoride). Equal amounts of protein, measured using either the Bio-Rad assay method (for cell pellets, $n = 3$ for each treatment group) (Bio-Rad, Hemel Hempstead, UK) or the bicinchonic acid reagent assay method (for tumor tissues, $n = 5$ for the control group and $n = 8$ for the LAQ824-treated group) (Pierce, Northumberland, UK) and bovine serum albumin as a standard, were loaded onto 12% (for cell pellets) or 4% to 12% (for tumor tissues) polyacrylamide gels. Cell lysate protein was transferred onto Immobilon-P membranes (Millipore, Bedford, MA), and tumor lysate protein was transferred onto polyvinylidene fluoride membranes. Blots were blocked in 5% nonfat milk for 2 hours and then incubated with primary anti–acetyl histone H3 antibody (Upstate, Charlottesville, VA), anti–C-RAF antibody (Santa Cruz Biotechnology, Santa Cruz, CA) or anti-Hsp70 (Stressgen Bioreagents, Ann Arbor, MI). This was followed by incubating the membranes with horseradish peroxidase–conjugated anti–rabbit secondary antibody for C-RAF and acetyl histone H3, and anti–mouse secondary antibody for Hsp70 (Amersham Biosciences, Buckinghamshire, UK). Equal gel loading was verified by incubating the blots with an anti–glyceraldehyde-3-phosphate dehydrogenase antibody (Chemicon, Hampshire, UK) or with β-actin (Abcam, Cambridge, UK) followed by an anti–mouse secondary antibody in 5% nonfat milk for 1 hour. Specific binding antibody–target protein interactions were detected using enhanced chemiluminescence plus reagents (Amersham Biosciences) and exposure to either Hyperfilm ECL (Amersham Biosciences) or X-OMAT Kodak (Rochester, NY) autoradiography film.

Immunohistochemistry

The microvessel density of HT29 tumors after vehicle and LAQ824 treatment was assessed by immunohistochemical staining for the vascular endothelial adhesion molecule, CD31. Snap-frozen tumor samples were sectioned and fixed in acetone. Sections were blocked in endogenous peroxidase (600 μl of 30% hydrogen peroxide in 100 ml of phosphate buffer solution) for 5 minutes and then incubated with primary CD31 antibody (01951D; PharMingen, Cambridge, UK) (diluted 1:50) for 35 minutes. The sections were further incubated in biotinylated rabbit anti–rat biotin (BA 5001; Vector Laboratories, Peterborough, UK) (diluted 1:100) for 35 minutes and followed by streptavidin horseradish peroxidase (P0397; Dako, Stockport, UK) (diluted 1:500) for a further 35 minutes. The sections were then finally developed in DAB, and nuclear counterstaining was performed with Harris' hematoxylin (Dako).

The method described by Qian et al. [25] was used for the microvessel density measurements. Briefly, analySIS (Soft Imaging System GmbH, Münster, Germany) was used to quantify the area occupied by the vessels in the histologic sections. The mean area per field from 10 fields per section (×200 = ×20 objective lens and ×10 ocular lens) was calculated and expressed as the mean percentage area occupied by blood vessels per field ± SEM. The experiment was repeated.

Histology

Part of the excised tumor was fixed in formal saline. Paraffin-embedded sections were cut and stained with Ehlich's hematoxylin and eosin (Dako) for the assessment of necrosis.

Cell Cycle Analysis

The effect of HDAC inhibition with LAQ824 and SAHA on cell cycle distribution was assessed in HT29 cells using flow cytometry and propidium iodide staining, as previously described [38].

Statistical Analysis

Data are presented as the mean ± SEM. For comparison of metabolite concentrations, metabolite ratios, and microvessel density, Student's standard t tests were used, with $P \le .05$ considered to be statistically significant. Pearson correlation was used to correlate changes in tumor volume and PME/total phosphorus (TotP) signal ratios, with $P \le 0.05$ considered to be statistically significant. All statistical tests were two-sided.

Results

Effect of HDAC Inhibition By SAHA and LAQ824 in HT29 Cells

Treatment of HT29 human colon carcinoma cells with SAHA and LAQ824 *in vitro* resulted in a significant antiproliferative effect with GI_{50} values for 96 hours' exposure of 1.7 ± 0.1 μM ($n = 3$) and 34.9 ± 1.3 nM ($n = 3$), respectively, as determined by the SRB assay. Exposure of HT29 cells *in vitro* to 34 μM SAHA and 350 nM LAQ824 for 24 hours in our MRS experiments led to a substantial reduction in cell count to 47 ± 5% ($P = .001$) and 50 ± 3% ($P = .0001$) of controls, respectively. Western blot analysis showed that acetyl histone H3 levels were markedly increased after exposure to both drugs consistent with HDAC inhibition (Figure 1 *A*). C-RAF decreased substantially, whereas Hsp70 levels remained unchanged after treatment (Figure 1 *A*). Flow cytometry indicated that HDAC inhibition with SAHA and LAQ824 was associated with significant alterations in cell cycle profiles. Exposure to SAHA and LAQ824 induced an accumulation in the G_1 phase from 25 ± 1% to 35 ± 1% ($n = 3$, $P = .009$) and 49 ± 3%, respectively ($n = 3$, $P = .007$). Furthermore, a reduction in the S-phase population (from 60 ± 2% to 20 ± 1%, $P = .0001$ and 21 ± 3%, $P = .0026$) and an increase in the G_2/M–phase populations (from 15 ± 1% to 45 ± 1%, $P = .0002$ and 30 ± 1%, $P = .0002$) were recorded after treatment with SAHA and LAQ824, respectively. Figure 2 *A* illustrates an example of ^{31}P MR spectra acquired from the aqueous fractions of extracts originating from control, SAHA-, and LAQ824-treated HT29 cells. ^{31}P MRS analysis indicated that inhibition of HDAC with LAQ824 and SAHA was associated with a significant increase of up to twofold in the levels of cellular PC (Table 1). Interestingly, no other significant alterations were observed in the spectra of cells exposed to either SAHA or LAQ824 (see Table 1).

Effect of LAQ824 on HT29 Xenografts In Vivo

Significant tumor growth inhibition was observed in HT29 xenografts after 2 days of LAQ824 treatment (25 mg/kg) when compared with vehicle-treated controls (Figure 1 *B*). The percentage inhibition was 72% at day 4, during which time the tumor volumes increased by 43 ± 5% in the vehicle-treated group and by 12 ± 3% in the LAQ824-treated group ($P = .0003$). The percentage inhibition was 46% at day 11, during which time the tumor volumes increased from day 1 by 209 ± 29% in the vehicle- and by 112 ± 18% in the LAQ824-treated group ($P < .0001$). This study also showed that significant tumor growth delay persisted for many days after the last dose of LAQ824 (Figure 1 *B*).

In vivo ^{31}P MR spectra from a HT29 tumor pre– and post–LAQ824 treatment are shown in Figure 2 *B*, where resonances from PME, PDE, Pi, α-, β-, γ-NTP, and phosphocreatine (PCr) can be observed. Marked decreases in NTP and PCr and an increase in Pi levels were found in LAQ824-treated tumors (Figure 2 *B*). This observation indicates that tumor bioenergetics is severely compromised after treatment. Statistically significant increases in PME/TotP ($P = .003$) and Pi/TotP ratios ($P = .0002$) and decreases in β-NTP/TotP ($P = .001$), β-NTP/Pi ($P = .003$), and PCr/TotP ($P = .004$) ratios and pHi ($P = .02$) were observed post–LAQ824 treatment (Table 2). No statistically significant change in the metabolite ratio was observed in the control (vehicle-treated) tumor group (Table 2).

Western blots of the excised tumors showed increased histone H3 acetylation in the LAQ824-treated group (Figure 1 *A*). These results confirm the expected inhibitory effect of LAQ824 on HDAC in HT29 xenografts. C-RAF expression decreased after LAQ824 treatment, but the expression of Hsp70 remained unchanged after treatment (Figure 1 *A*).

Relationship Between PME/TotP Ratios and Tumor Response

We examined the degree of association between PME/TotP ratio and tumor response. This was done by comparing the individual % change in PME/TotP (posttreatment ratio relative to pretreatment ratio) ratios from the cohorts of vehicle- and LAQ824-treated tumors with their corresponding % change in tumor volumes (posttreatment volume relative to pretreatment volume). A statistically significant inverse correlation was found between percentage increase in PME/TotP ratio and percentage change in tumor volume ($r = –0.61$, $P = .01$) (Figure 3).

Effect of LAQ824 on HT29 Tumor Extracts

In vitro ^{31}P MRS analysis of extracts of the HT29 tumor xenografts allows better resolution of the metabolite signals than is possible *in vivo*. Increased levels of PC ($P = .04$), PE ($P = .02$), and Pi ($P = .06$) and decreased levels of GPC ($P = .01$) and GPE ($P = .05$) were detected in LAQ824-treated tumors (Table 3 *A*) relative to controls, confirming our *in vivo* ^{31}P MRS findings.

In vitro ^{1}H MR spectra (expanded from 0.5 to 5.5 ppm) of the HT29 tumor extracts from a control vehicle-treated and a LAQ824-treated mouse are illustrated in Figure 2 *C*, respectively, showing resonances from leucine, *iso*-leucine, valine, lactate, alanine, acetate, glutamine, glutamate, creatine, PCr, free choline, PC, GPC, taurine, glycine, and glucose [47]. Elevated PC ($P = .04$), free choline ($P = .01$), leucine ($P = .005$), *iso*-leucine ($P = .005$), and valine ($P = .04$) levels and reduced GPC ($P = .02$), glutamate ($P = .04$), glutamine ($P = .03$), glucose ($P = .001$), and PCr and creatine ($P = .05$) levels were found in LAQ824-treated HT29 tumor extracts when compared with vehicle-treated tumor extracts (Table 3 *B*).

Histologic and Vascular Effect of LAQ824 on HT29 Xenografts

Histologic sections of a control and a LAQ824-treated HT29 tumor are shown in Figure 1 *C*. LAQ824-treated tumors showed extensive necrosis when compared with vehicle controls.

Microvessel density in vehicle- and LAQ824-treated HT29 tumors was assessed by immunohistochemical staining for CD31. A marked reduction of CD31 staining and a significant decrease by 67% in microvessel density was found in LAQ824-treated tumors (25 mg/kg for 2 days) when compared with controls ($P = .007$; Figure 1, *C* and *D*).

Discussion

Pharmacodynamic and tumor response biomarkers are increasingly important for the development of new molecular therapeutics [27–29]. Histone deacetylase inhibition causes increased or decreased expression of a variety of genes that mediate proliferation, cell cycle progression, angiogenesis, and apoptosis [7–19] and perturb the acetylation status of many proteins in addition to histones [19–24]. Tumor response to LAQ824 can be assessed using molecular biologic markers, particularly the induction of histone H3 and H4 hyperacetylation [22–26] and the depletion of Hsp90 client proteins, such as C-RAF. However, a noninvasive, direct, or surrogate marker of tumor response to this novel treatment would be of value [27].

In our study, inhibition of HDAC in HT29 cells by LAQ824 or SAHA was demonstrated by the induction of histone H3 acetylation using Western blot analysis. The reduction in expression of the Hsp90 client protein, C-RAF, is consistent with Hsp90 inhibition after exposure to HDAC inhibitors [19,21–24,48,49]. However, the induction of Hsp70 expression, which is also a marker of Hsp90 inhibition [49], was not observed in our cell and tumor samples. This observation has also been reported previously in prostate cancer cells after HDAC inhibition with a SAHA analog [48], and the explanation for this finding remains unknown. This may result from a direct inhibitory effect of HDAC inhibition on Hsp70 induction.

The molecular signature of HDAC inhibition as defined by the above changes in the HT29 cell line, and in previous studies [13,24–26,40], was also seen in the HT29 xenografts. Growth inhibition was observed in both HT29 cells and tumors. Flow cytometry of HT29 cells treated with SAHA or LAQ824 showed significant alterations in cell cycle distributions when compared with controls. Both drugs induced a G_1- and a G_2/M–phase accumulation as well as a reduction in the S-phase population. This observation indicates cell cycle arrest after HDAC inhibition and is consistent with the reported effect of HDAC inhibition on cell cycle progression [10,11,24,26,48].

The primary aim of this project was to develop a noninvasive ^{31}P MRS marker of response to the HDAC inhibitor LAQ824. To facilitate this, we looked for metabolite changes indicative of tumor response both *in vitro* (HT29 cells) and *in vivo* (HT29 xenografts). Concentrations used on HT29 cells *in vitro* were those that caused around 50% cell growth inhibition over 24 hours and an increase in histone acetylation. The dose used to treat HT29 tumors *in vivo* was well tolerated (as no significant weight loss was found after treatment) and caused tumor growth inhibition, again with evidence of target modulation shown by an increase in histone acetylation. HT29 cells

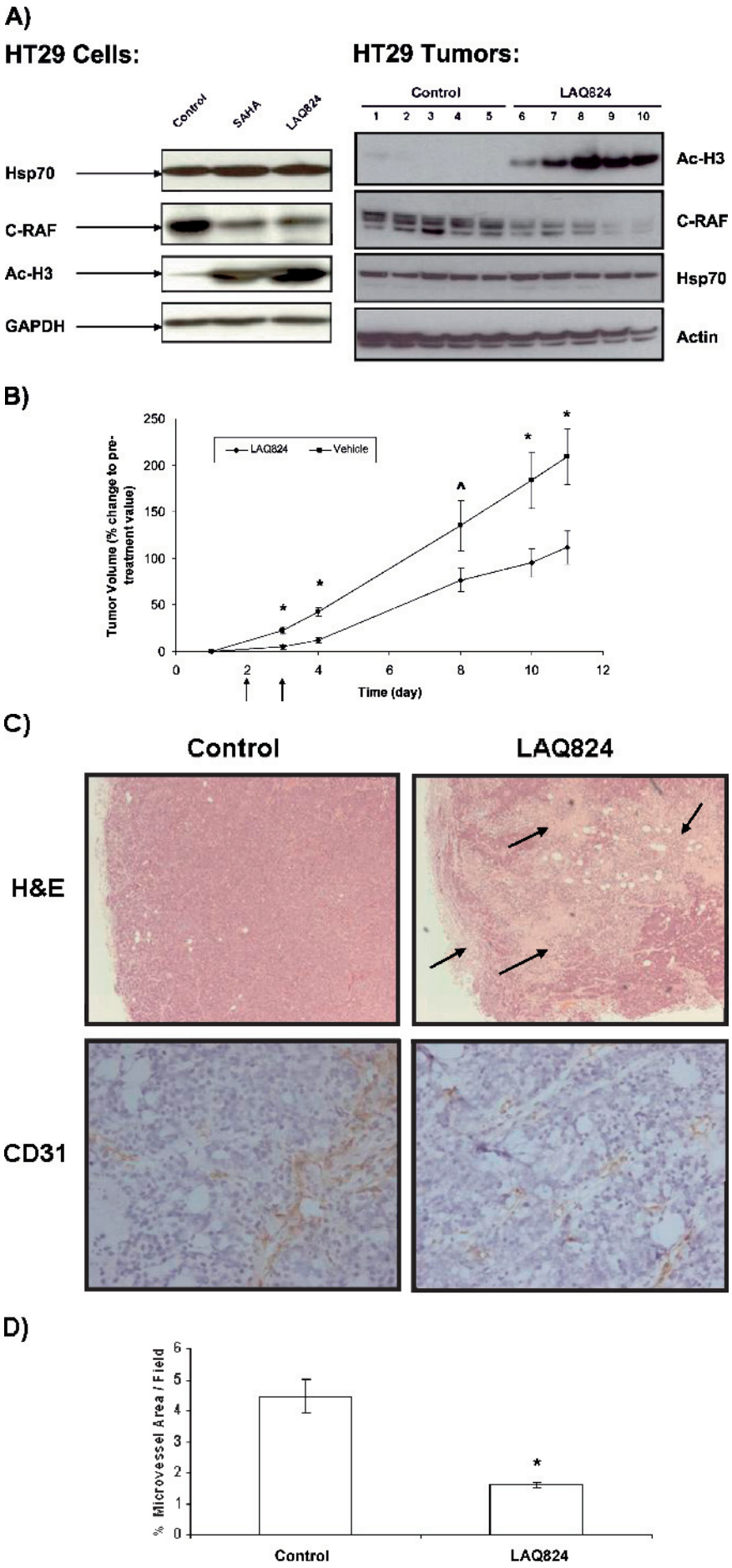
A)
HT29 Cells:
Control
SAHA
LAQ824
Hsp70
C-RAF
Ac-H3
GAPDH
HT29 Tumors:
Control
LAQ824
1 2 3 4 5 6 7 8 9 10
Ac-H3
C-RAF
Hsp70
Actin
B)
LAQ824
Vehicle
Tumor Volume (% change to pre-treatment value)
Time (day)
C)
Control
LAQ824
H&E
CD31
D)
% Microvessel Area / Field
Control
LAQ824

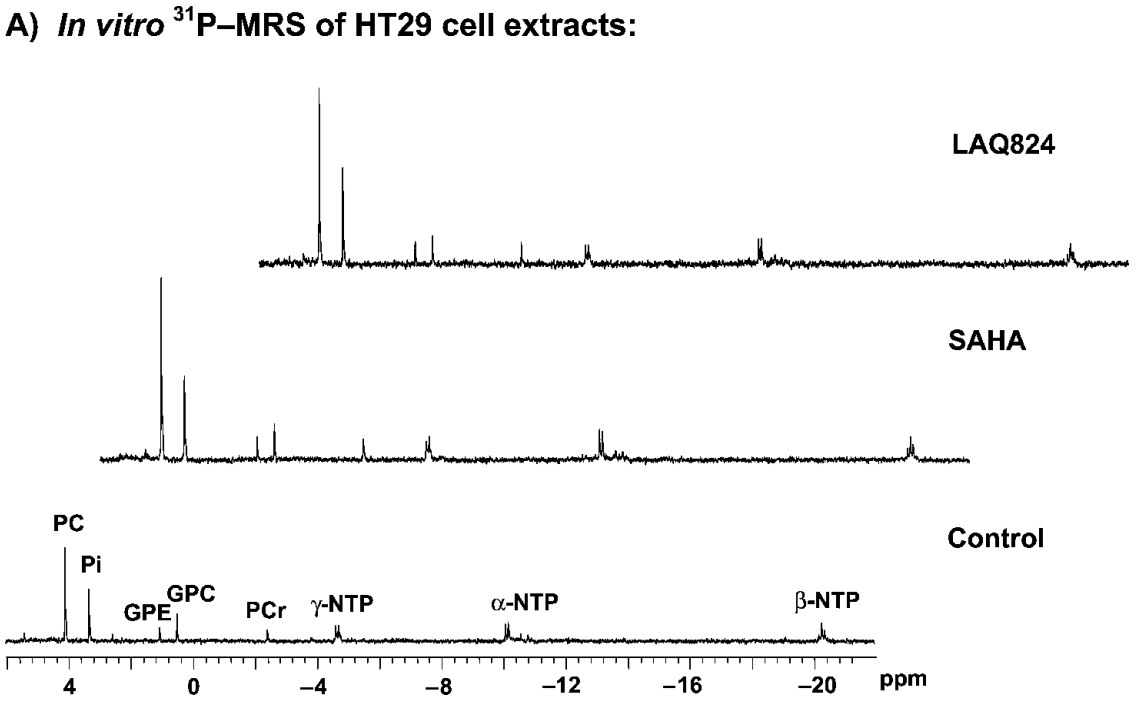

Figure 2. Inhibitions of HDAC by LAQ824 are associated with a significant drop in tumor bioenergetics and increase in phosphomonoesters and phosphocholine levels. (A) *In vitro* ^{31}P MRS of an HT29 cell extract treated with: vehicle (bottom panel), 34 μM SAHA (middle panel), and 350 nM LAQ824 (top panel) for 24 hours. Peak assignments: phosphocholine (PC), glycerophosphocholine (GPC), glycerophosphoethanolamine (GPE), inorganic phosphate (Pi), phosphocreatine (PCr), and nucleoside triphosphates (α-, β-, γ-NTP). (B) *In vivo* ^{31}P MR spectra of a HT29 tumor before (top panel) and after (bottom panel) LAQ824 treatment (25 mg/kg i.p. for 2 days) are shown. Peak assignments: phosphomonoesters (PME), phosphodiesters (PDE), inorganic phosphate (Pi), phosphocreatine (PCr), and nucleoside triphosphates (α-, β-, γ-NTP). (C) *In vitro* ^{1}H MR spectra of vehicle- (top panel) and LAQ824-treated (bottom panel) HT29 tumor extracts are illustrated. Peak assignments: leucine (1), *iso*-leucine (2), valine (3), lactate (4), alanine (5), acetate (6), glutamate (7), glutamine (8), dimethylamine (9), creatine + phosphocreatine (10), free choline (11), phosphocholine (12), glycerophosphocholine (13), taurine (14), glycine (15), creatine (16), phosphocreatine (17), water (18), glucose (19).

treated with HDAC inhibitors (LAQ824 and SAHA) showed a statistically significant increase in PC levels. In the HT29 xenograft model, we also observed a significant MRS-detectable increase in the PME peak (with contributions from both PC and PE) post–LAQ824 treatment. A significant correlation was also found between the increased PME/TotP ratio and tumor response. The principal sources of PME signals in tumors are PC and PE, precursors of phosphatidylcholine and phosphatidylethanolamine, which are major components of biologic membranes [50]. This increase in PME is confirmed by the significant rises in PC and PE levels observed in ^{1}H and ^{31}P MR spectra of LAQ824-treated tumor extracts when compared with controls. These results are consistent with findings from a recent study in a human prostate cancer (PC3) cell line, which also showed (using *in vitro* MRS of cell extracts) that PC levels increase after HDAC inhibition with a SAHA analog [48], indicating that these observations are not cell line–specific or tissue type–dependent.

Figure 1. LAQ824 causes induction of histone acetylation and reduction of C-RAF expression, tumor growth delay, extensive tumor necrosis, and reduction of microvessel density in HT29 tumor model. (A) Western blots for Hsp70 and C-RAF expression and histone (H3) acetylation are shown in HT29 cells after treatment with vehicle (left lane), 34 μM SAHA [20 × GI_{50}] (middle lane), and 350 nM LAQ824 [10 × GI_{50}] (right lane) for 24 hours (left panel). Western blots for histone (H3) acetylation and C-RAF and Hsp70 expression are shown in HT29 xenografts following daily (×2) i.p. injection of vehicle (10% DMSO and 90% of 5% dextrose in water) (lanes 1–5) and 25 mg/kg LAQ824 i.p. (lanes 6–10) (right panel). (B) Percentage change in tumor volumes (tumor volume post–LAQ824 or –vehicle treatment relative to pretreatment volume) over time are shown in HT29 xenografts following daily (×2) i.p. injection of vehicle (10% DMSO and 90% of 5% dextrose in water) and 25 mg/kg LAQ824 i.p. Vehicle-treated (filled squares; $n = 18$ at days 1, 3, and 4 and $n = 5$ at days 8, 10, and 11) and LAQ824-treated group (filled diamonds; $n = 20$ at days 1, 3, and 4 and $n = 5$ at days 8, 10, and 11) are shown in the graph. Treatment days are shown by black arrows. Results are expressed as mean ± SEM. Two-tailed unpaired *t* test was used to compare changes between the vehicle- and LAQ824-treated groups. $^{*}P \leq .03$ and $^{\wedge}P = .08$ when comparing LAQ824-treated with vehicle controls. (C) Hematoxylin and eosin (H&E) staining for necrosis (top panels; original magnification, ×40) and immunohistochemical staining of CD31 for endothelial cells are shown (blood vessels are in brown) (bottom panels; original magnification, ×200) in HT29 xenografts after daily (×2) i.p. injection of vehicle (10% DMSO and 90% of 5% dextrose in water) (left panels) and 25 mg/kg LAQ824 i.p. (right panels). Some areas of necrosis are shown by the black arrows. (D) Quantitative analysis of microvessel density was performed in LAQ824- and vehicle-treated tumors using analySIS (Soft Imaging System GmbH). Results are expressed as percent microvessel area per field, mean ± SEM. Two-tailed unpaired *t* test was used to compare changes between the vehicle- ($n = 2$) and LAQ824-treated groups ($n = 3$). $^{*}P = .007$ when comparing LAQ824-treated with vehicle controls.

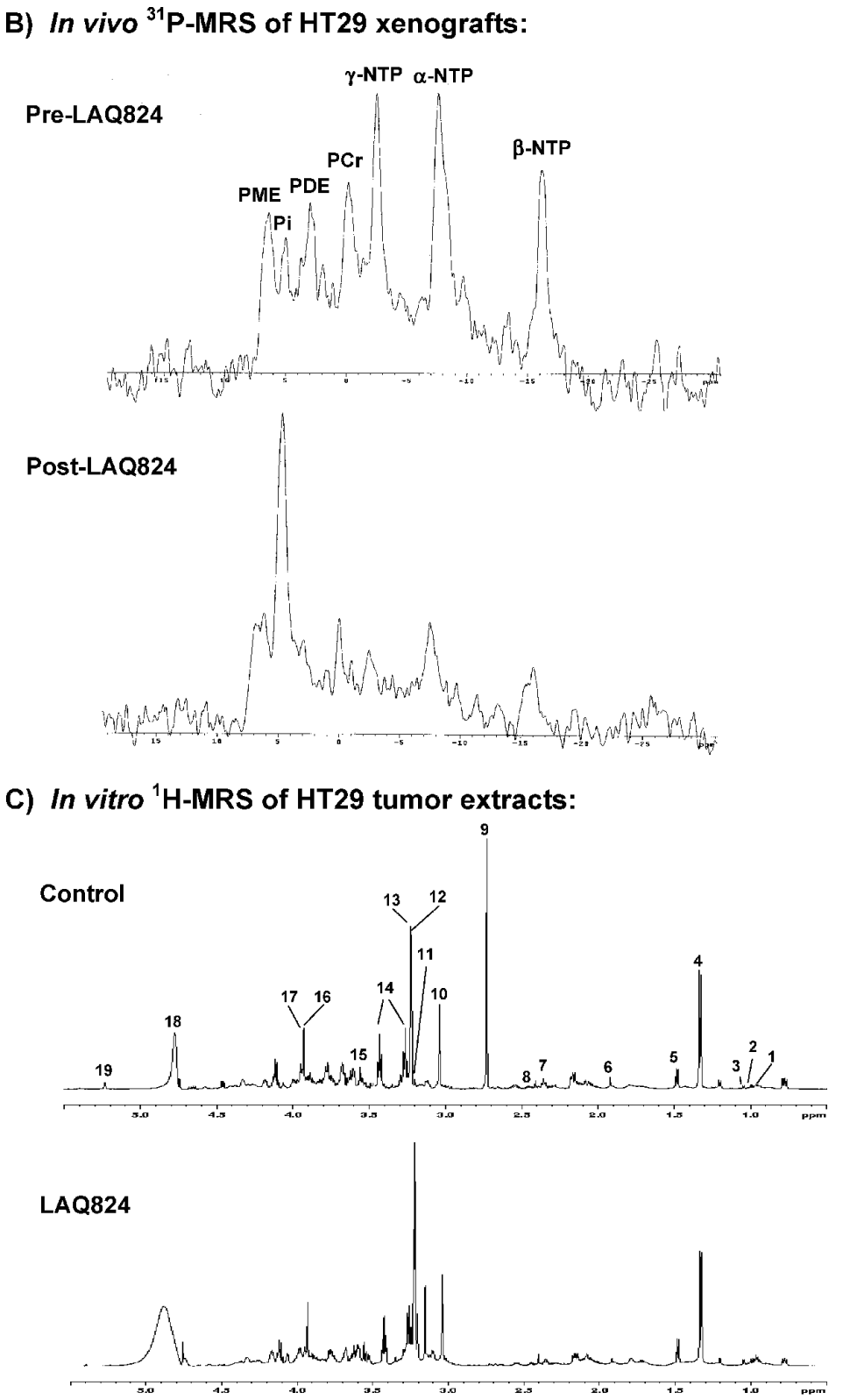

Figure 2. (*continued*)

Although both PC and PE peaks were observed in untreated tumor extracts, only the PC peak was observed in the cultured cell extracts. Similar findings [51] in HT29 tumor xenografts and cultured cells have been attributed to the greater availability of ethanolamine *in vivo* when compared with cells in culture, where ethanolamine is only present in added serum. The relative amounts of PC and PE, both of which contribute to the PME signal, appear to vary among both experimental models and human tumors in patients [52].

It is possible that other agents with HDAC inhibitory properties could produce different results, e.g., Milkevitch et al. [53] reported a

Table 1. The Effect of Treatment with SAHA and LAQ824 on the ^{31}P MRS Detectable Aqueous Metabolites of HT29 Human Colon Carcinoma Cells (N = 4).

Metabolites	Control	LAQ824	SAHA
PC	19 ± 1	38 ± 5*	42 ± 4†
GPC	7 ± 1	6 ± 1	7 ± 1
GPE	3 ± 1	5 ± 1	5 ± 1
NTP	9 ± 1	13 ± 3	12 ± 2

Metabolite content is expressed as femtomole per cell. Data are expressed as mean ± SEM.
Two-tailed unpaired t test was used to compare changes between the vehicle-, SAHA-, and LAQ824-treated groups: *P = .04 and †P = .01.
PC indicates phosphocholine; *GPE*, glycerophosphoethanolamine; *GPC*, glycerophosphocholine; *NTP*, nucleoside triphosphate.

rise in GPC in prostate cancer cells *in vitro* after treatment with phenylbutyrate. This may have been because this agent is less selective than SAHA and LAQ824 as an inhibitor of HDACs or to differences in the *in vitro* culture conditions.

In vitro increases in PC have been observed in two different cancer lines (HT29 and PC3 [48]) with two different HDAC inhibitors (SAHA and LAQ824), and *in vivo* increases in PME (after LAQ824 treatment) have also been found. It would be possible to measure these PME and PC changes (as total choline) *in vivo* by ^{1}H MRS as a potential biomarker. For ease of measurement, the ^{1}H MRS measurements were limited to tumor extracts in this study.

As mentioned, the depletion of C-RAF after HDAC inhibition is consistent with Hsp90 inhibition after exposure to HDAC inhibitors. Thus, it is of interest that HDAC inhibition also results in increased PC and PME levels, because similar molecular and spectral changes were found in HT29 cells and in xenografts after treatment with the Hsp90 inhibitor 17-allylamino,17-demethoxygeldanamycin [36]. The basis for the increased levels of PC and PME warrants further investigation, but it appears that Hsp90 modulation may be implicated. Phospholipid changes have previously been attributed to the modulation of various signaling pathways [38,39].

Marked and significant decreases in high-energy phosphates (β-NTP/TotP, β-NTP/Pi, and PCr/TotP ratios) and pHi and an increase

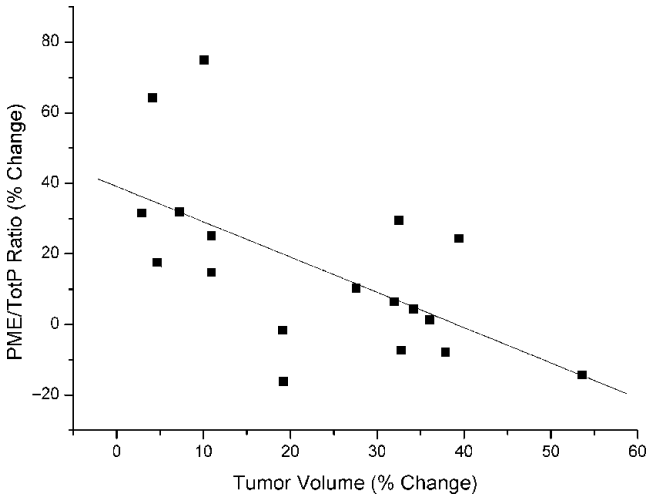

Figure 3. The increased PME/TotP ratio was correlated with tumor response. The percentage change in PME/TotP ratios (posttreatment values relative to pretreatment values) is plotted against percentage change in tumor volumes (posttreatment values relative to pretreatment values). *Solid line* indicates linear regression line: $r = -0.61$, $P = .01$.

in a low-energy phosphate (Pi/TotP ratio) were observed in HT29 tumors post–LAQ824 treatment. These changes suggest that tumor bioenergetics is severely compromised after treatment. This dramatic drop in tumor bioenergetics after treatment of LAQ824 has not been reported previously. These *in vivo* bioenergetic changes and *in vitro* metabolic changes (as detected by *in vitro* ^{1}H and ^{31}P MRS of tumor extracts) are consistent with a reduced perfusion in HT29 tumors after treatment with LAQ824. Indeed, similar dramatic effects on tumor bioenergetics were reported in HT29 tumors after treatment

Table 2. *In Vivo* ^{31}P Magnetic Resonance Spectroscopy of HT29 Tumors.

(A) Pre– and Post–Vehicle Treatment (N = 7)

Metabolite Ratios	Pre-Vehicle	Post-Vehicle	P†
PME/TotP	0.18 ± 0.01	0.18 ± 0.02	NS
β-NTP/TotP	0.21 ± 0.01	0.21 ± 0.01	NS
PCr/TotP	0.10 ± 0.01	0.09 ± 0.02	NS
β-NTP/Pi	3.15 ± 0.55	2.50 ± 0.35	NS
Pi/TotP	0.06 ± 0.03	0.09 ± 0.01	NS
pHi	7.12 ± 0.06	7.14 ± 0.06	NS

(B) Pre– and Post–LAQ824 Treatment (N = 11)

Metabolite ratios	Pre-LAQ824	Post-LAQ824	P
PME/TotP	0.18 ± 0.01	0.23 ± 0.01	.003
β-NTP/TotP	0.21 ± 0.01	0.13 ± 0.02	.001
PCr/TotP	0.08 ± 0.01	0.04 ± 0.01	.004
β-NTP/Pi	2.62 ± 0.33	1.09 ± 0.43	.003
Pi/TotP	0.09 ± 0.01	0.21 ± 0.03	.0002
pHi	7.08 ± 0.03	6.93 ± 0.04	.02

Data are expressed as mean ± SEM.
PME indicates phosphomonoester; *TotP*, total phosphorus signal; *β-NTP*, β-nucleoside triphosphate; *Pi*, inorganic phosphate; *pHi*, intracellular pH; *PCr*, phosphocreatine; *NS*, not statistically significant (P > .1).
†Two-tailed paired t test was used to compare changes pre– and post–LAQ824 treatment within the same group of animals.

Table 3. *In Vitro* Magnetic Resonance Spectroscopy of HT29 Tumor Extracts Following Vehicle and LAQ824 Treatment.

Metabolites (μmol/g wet weight)	Control (N = 5)	LAQ824 (N = 5)	P†
(A) Phosphorus MRS			
PE	1.13 ± 0.20	1.85 ± 0.09	.02
PC	1.87 ± 0.21	2.72 ± 0.21	.04
GPE	1.66 ± 0.44	0.49 ± 0.10	.05
GPC	2.34 ± 0.33	0.81 ± 0.08	.01
Pi	5.01 ± 0.91	9.00 ± 1.23	.06
(B) Proton MRS			
PC	1.76 ± 0.16	2.51 ± 0.25	.04
GPC	2.05 ± 0.23	1.26 ± 0.13	.02
Free choline	0.16 ± 0.03	0.49 ± 0.08	.01
Leucine	0.23 ± 0.03	0.41 ± 0.08	.005
Iso-leucine	0.11 ± 0.02	0.22 ± 0.02	.005
Valine	0.26 ± 0.04	0.39 ± 0.04	.04
Glutamate	2.05 ± 0.35	0.97 ± 0.09	.04
Glutamine	0.88 ± 0.11	0.44 ± 0.12	.03
PCr + Cr	5.19 ± 0.70	2.40 ± 0.99	.05
Glucose	0.95 ± 0.06	0.37 ± 0.08	.001
Lactate	6.84 ± 0.79	5.80 ± 2.24	NS
Alanine	1.82 ± 0.26	2.05 ± 0.10	NS
Taurine	6.91 ± 0.82	5.17 ± 0.42	NS
Glycine	1.46 ± 0.18	1.23 ± 0.05	NS

Data are expressed as mean ± SEM.
PE indicates phosphoethanolamine; *PC*, phosphocholine; *GPE*, glycerophosphoethanolamine; *GPC*, *glycerophosphocholine*; *PCr*, phosphocreatine; *Cr*, creatine; *Pi*, inorganic phosphate; *NS*, not statistically significant (P > .1).
†Two-tailed unpaired t test was used to compare changes between the vehicle- and LAQ824-treated groups.

with the vascular disrupting agent, 5,6-dimethylxanthenone-4-acetic acid [54].

Surprisingly, no significant change in lactate was found in LAQ824-treated tumor extracts when compared with vehicle-treated controls, as one may expect an increase in tumor lactate when tumor perfusion is reduced. This observation has also been previously reported in xenografts treated with a vascular disrupting agent, ZD6126 [55], and the explanation for this finding remains unclear.

To confirm whether LAQ824 exerts a vascular effect in HT29 tumor xenografts, immunohistochemical staining of the vascular endothelial adhesion molecule, CD31, was carried out on frozen sections of vehicle- and LAQ824-treated tumors. A significant reduction in microvessel density was found in LAQ824-treated tumors when compared with vehicle controls; this finding, together with extensive necrosis and a dramatic drop in tumor bioenergetics, is consistent with the hypothesis that LAQ824 reduces perfusion in HT29 tumors. A reduction in microvessel density was also previously reported in LAQ824-treated PC3 and MDA-MB231 tumors, where LAQ824 treatment was found to inhibit the expression of angiogenesis-related genes, such as *angiopoietin-2*, *Tie-2*, and *survivin* in endothelial cells, and downregulation of HIF-1α and VEGF expression in tumor cells [25]. Weinberg [56] has recently suggested that the effectiveness of conventional chemotherapeutics may be strongly influenced by the sensitivity of the tumor-associated microvasculature to these agents. This dual action of LAQ824 appears to be an example of such an effect.

The reduction in perfusion observed in LAQ824-treated tumors is likely to cause tumors to become deprived of essential nutrients. This may explain the dramatic drop in *in vivo* tumor bioenergetics and significant decrease in glucose, PCr + Cr, glutamine, and glutamate levels (these metabolites may be used by the tumor to produce energy when the nutrient supply is low) observed through *in vitro* ^{1}H MRS of tumor extracts.

In vitro ^{1}H and ^{31}P MRS of LAQ824-treated tumor extracts also showed significant decreases in GPE and GPC and increased choline levels. These phospholipid changes have also been observed after treatment of HT29 tumors with the vascular disruptive agent, 5,6-dimethylxanthenone-4-acetic acid [54]. Choline-containing metabolites are associated with membrane metabolism, and changes in the concentration of these metabolites may indicate changes in membrane turnover. The significant drop in GPC and GPE (membrane degradation products) and significant rise in free choline (not membrane-bound) after LAQ824 treatment suggests that LAQ824 may cause a reduction in membrane turnover and thus growth inhibition.

An increase in branched-chain amino acids (i.e., leucine, *iso*-leucine, and valine) was observed in ^{1}H MRS of LAQ824-treated tumor extracts. This observation suggests a reduction in protein synthesis in HT29 tumors after treatment. Therefore, the vascular effects induced by LAQ824 cause severe disruption of essential nutrients being transported to the tumor, which then induces a depletion of energy within the tumor and leads to a decrease in tumor growth.

The impairment in tumor bioenergetics and many metabolic changes observed in tumor extracts are not observed *in vitro*, in cell studies. This is consistent with the hypothesis that these changes are likely to be linked to the vascular effects of LAQ824 on solid tumors [25]. Cultured tumor cells are bathed in well-oxygenated medium containing sufficient levels of nutrients, whereas, *in vivo*, the structurally and functionally disturbed microcirculation is likely to impair the delivery of nutrients and oxygen [57,58]. This could lead to dysfunctional energy metabolism manifested by decreases in tumor bioenergetics.

In conclusion, the present study has identified two potential noninvasive surrogate biomarkers for the action of LAQ824: (1) a decrease in tumor bioenergetics and (2) an increase in PME. Similar effects of LAQ824 on PC and PME levels were found to occur in cultured cells *in vitro*, in tumor xenografts *in vivo*, and in tumor extracts *in vitro*. The increased PME/TotP ratio, which was only observed *in vivo*, was found to correlate with tumor response, indicating that it could act as a potential pharmacodynamic biomarker of drug activity. Hence, monitoring the pharmacodynamic effects of LAQ824 treatment and possibly of other HDAC inhibitors on tumor phospholipid metabolism by ^{31}P MRS may provide noninvasive surrogate markers for HDAC inhibition and potentially of response in solid tumors in clinical trials.

Acknowledgments

The authors thank the Biomics Centre at St. George's University of London for the use of the 600-MHz NMR system and Mrs. Jenny Titley from the Institute for Cancer Research for her help with the FACS analysis.

References

[1] Legube G and Trouche D (2003). Regulating histone acetyltransferases and deacetylases. *EMBO Rep* **4**, 944–947.

[2] Struhl K (1998). Histone acetylation and transcriptional regulatory mechanisms. *Genes Dev* **12**, 599–606.

[3] Sengupta N and Seto E (2004). Regulation of histone deacetylase activities. *J Cell Biochem* **93**, 57–67.

[4] Marks P, Rifkind RA, Richon VM, Breslow R, Miller T, and Kelly WK (2001). Histone deacetylases and cancer: causes and therapies. *Nat Rev Cancer* **1**, 194–202.

[5] Schagdarsurengin U, Gimm O, Hoang-Vu C, Dralle H, Pfeifer GP, and Dammann R (2002). Frequent epigenetic silencing of the CpG island promoter of RASSF1A in thyroid carcinoma. *Cancer Res* **62**, 3698–3701.

[6] van Engeland M, Roemen GM, Brink M, Pachen MM, Weijenberg MP, de Bruïne AP, Arends JW, van den Brandt PA, de Goeij AF, and Herman JG (2002). K-*ras* mutations and RASSF1A promoter methylation in colorectal cancer. *Oncogene* **21**, 3792–3795.

[7] Kim MS, Kwon HJ, Lee YM, Baek JH, Jang JE, Lee SW, Moon EJ, Kim HS, Lee SK, Chung HY, et al. (2001). Histone deacetylases induce angiogenesis by negative regulation of tumor suppressor genes. *Nat Med* **7**, 437–443.

[8] Kristeleit R, Stimson L, Workman P, and Aherne W (2004). Histone modification enzymes: novel targets for cancer drugs. *Expert Opin Emerg Drugs* **9**, 135–154.

[9] Marks PA, Richon VM, and Rifkind PA (2000). Histone deacetylase inhibitors: inducers of differentiation or apoptosis of transformed cells. *J Natl Cancer Inst* **92**, 1210–1216.

[10] Strait KA, Warnick CT, Ford CD, Dabbas B, Hammond EH, and Ilstrup SJ (2005). Histone deacetylase inhibitors induce G2-checkpoint arrest and apoptosis in cisplatinum-resistant ovarian cancer cells associated with overexpression of the Bcl-2–related protein Bad. *Mol Cancer Ther* **4**, 603–611.

[11] Maeda T, Nagaoka Y, Kawai Y, Takagaki N, Yasuda C, Yogosawa S, Sowa Y, Sakai T, and Uesato S (2005). Inhibitory effects of cancer cell proliferation by novel histone deacetylase inhibitors involve p21/WAF1 induction and G(2)/M arrest. *Biol Pharm Bull* **28**, 849–853.

[12] Jeong JW, Bae MK, Ahn MY, Kim SH, Sohn TK, Bae MH, Yoo MA, Song EJ, Lee KJ, and Kim KW (2002). Regulation and destabilization of HIF-1α by ARD1-mediated acetylation. *Cell* **111**, 709–720.

[13] Qian DZ, Kachhap SK, Collis SJ, Verheul HM, Carducci MA, Atadja P, and Pili R (2006). Class II histone deacetylases are associated with VHL-independent regulation of hypoxia-inducible factor 1α. *Cancer Res* **66**, 8814–8821.

[14] Mie LY, Kim SH, Kim HS, Jin Son M, Nakajima H, Jeong Kwon H, and Kim KW (2003). Inhibition of hypoxia-induced angiogenesis by FK228, a specific histone deacetylase inhibitor, via suppression of HIF-1α activity. *Biochem Biophys Res Commun* **300**, 241–246.

[15] Han JW, Ahn SH, Park SH, Wang SY, Bae GU, Seo DW, Kwon HK, Hong S, Lee HY, Lee YW, et al. (2000). Apicidin, a histone deacetylase inhibitor, inhibits proliferation of tumor cells via induction of p21WAF1/Cip1 and gelsolin. *Cancer Res* **60**, 6068–6074.

[16] Deroanne CF, Bonjean K, Serotte S, Devy L, Colige A, Clausse N, Blacher S, Verdin E, Foidart JM, Nusgens BV, et al. (2002). Histone deacetylases inhibitors as anti-angiogenic agents altering vascular endothelial growth factor signaling. *Oncogene* **21**, 427–436.

[17] Rossig L, Li H, Fisslthaler B, Urbich C, Fleming I, Förstermann U, Zeiher AM, and Dimmeler S (2002). Inhibitors of histone deacetylation downregulate the expression of endothelial nitric oxide synthase and compromise endothelial cell function in vasorelaxation and angiogenesis. *Circ Res* **91**, 837–844.

[18] Scott GK, Marden C, Xu F, Kirk L, and Benz CC (2002). Transcriptional repression of ErbB2 by histone deacetylase inhibitors detected by a genomically integrated ErbB2 promoter–reporting cell screen. *Mol Cancer Ther* **1**, 385–392.

[19] Drummond DC, Noble CO, Kirpotin DB, Guo Z, Scott GK, and Benz CC (2005). Clinical development of histone deacetylase inhibitors as anticancer agents. *Annu Rev Pharmacol Toxicol* **45**, 495–528.

[20] McCabe MT, Azih OJ, and Day ML (2005). pRb-independent growth arrest and transcriptional regulation of E2F target genes. *Neoplasia* **7**, 141–151.

[21] Bali P, Pranpat M, Bradner J, Balasis M, Fiskus W, Guo F, Rocha K, Kumaraswamy S, Boyapalle S, Atadja P, et al. (2005). Inhibition of histone deacetylase 6 acetylates and disrupts the chaperone function of heat shock protein 90: a novel basis for antileukemia activity of histone deacetylase inhibitors. *J Biol Chem* **280**, 26729–26734.

[22] Chen L, Meng S, Wang H, Bali P, Bai W, Li B, Atadja P, Bhalla KN, and Wu J (2005). Chemical ablation of androgen receptor in prostate cancer cells by the histone deacetylase inhibitor LAQ824. *Mol Cancer Ther* **4**, 1311–1319.

[23] Nimmanapalli R, Fuino L, Bali P, Gasparetto M, Glozak M, Tao J, Moscinski L, Smith C, Wu J, Jove R, et al. (2003). Histone deacetylase inhibitor LAQ824 both lowers expression and promotes proteasomal degradation of Bcr-Abl and induces apoptosis of imatinib mesylate-sensitive or -refractory chronic myelogenous leukemia–blast crisis cells. *Cancer Res* **63**, 5126–5135.

[24] Atadja P, Gao L, Kwon P, Trogani N, Walker H, Hsu M, Yeleswarapu L, Chandramouli N, Perez L, Versace R, et al. (2004). Selective growth inhibition of tumor cells by a novel histone deacetylase inhibitor, NVP-LAQ824. *Cancer Res* **64**, 689–695.

[25] Qian DZ, Wang X, Kachhap SK, Kato Y, Wei Y, Zhang L, Atadja P, and Pili R (2004). The histone deacetylase inhibitor NVP-LAQ824 inhibits angiogenesis and has a greater antitumor effect in combination with the vascular endothelial growth factor reception tyrosine kinase inhibitor PTK787/ZK222584. *Cancer Res* **64**, 6626–6634.

[26] Leyton J, Alao JP, Da Costa M, Stavropoulou AV, Latigo JR, Perumal M, Pillai R, He Q, Atadja P, Lam EW, et al. (2006). *In vivo* biological activity of the histone deacetylase inhibitor LAQ824 is detectable with 3′-deoxy-3′-[^{18}F] fluorothymidine positron emission tomography. *Cancer Res* **66**, 7621–7629.

[27] Workman P, Aboagye EO, Chung Y-L, Griffiths JR, Hart R, Leach MO, Maxwell RJ, McSheehy PMJ, Price PM, and Zweit J (2006). Minimally-invasive pharmacokinetic and pharmacodynamic technologies in hypothesis—testing clinical trials of innovative therapies. *J Natl Cancer Inst* **98**, 580–598.

[28] Workman P (2002). Challenges of PK/PD measurements in modern drug development. *Eur J Cancer* **38**, 2189–2193.

[29] Workman P (2003). How much gets there and what does it do?: The need for better pharmacokinetic and pharmacodynamic endpoints in contemporary drug discovery and development. *Curr Pharm Des* **9**, 891–902.

[30] Parulekar WR and Eisenhauer EA (2004). Phase I trial design for solid tumor studies of targeted, non-cytotoxic agents: theory and practice. *J Natl Cancer Inst* **96**, 990–997.

[31] Webb GA, Ed (2006). *Modern Magnetic Resonance. Part II: Applications in Medical and Pharmaceutical Sciences.* New York, Springer.

[32] Arias-Mendoza F, Payne GS, Zakian KL, Schwarz AJ, Stubbs M, Stoyanova R, Ballon D, Howe FA, Koutcher JA, Leach MO, et al. (2006). *In vivo* ^{31}P MR spectral patterns and reproducibility in cancer patients studied in a multi-institution trial. *NMR Biomed* **19**, 504–512.

[33] Galbraith SM (2006). MR in oncology drug development. *NMR Biomed* **19**, 681–689.

[34] Leach MO, Verrill M, Glaholm J, Smith TA, Collins DJ, Payne GS, Sharp JC, Ronen SM, McCready VR, Powles TJ, et al. (1998). Measurements of human breast cancer using magnetic resonance spectroscopy: a review of clinical measurements and a report of localized ^{31}P measurements of response to treatment. *NMR Biomed* **11**, 314–340.

[35] Aboagye EO, Dillehay LE, Bhujwalla ZM, and Lee D-J (1998). Hypoxic cell cytotoxin tirapazamine induces acute changes in tumor energy metabolism and pH: a ^{31}P magnetic resonance spectroscopy study. *Radiat Oncol Investig* **6**, 249–254.

[36] Chung YL, Troy H, Banerji U, Jackson LE, Walton MI, Stubbs M, Griffiths JR, Judson IR, Leach MO, Workman P, et al. (2003). Magnetic resonance spectroscopic pharmacodynamic markers of the heat shock protein 90 inhibitor 17-allylamino,17-demethoxygeldanamycin (17AAG) in human colon cancer models. *J Natl Cancer Inst* **95**, 1624–1633.

[37] Al-Saffar NMS, Troy H, Ramirez de Molina A, Jackson LE, Madhu B, Griffiths JR, Leach MO, Workman P, Lacal JC, Judson IR, et al. (2006). Noninvasive magnetic resonance spectroscopic pharmacodynamic markers of the choline kinase inhibitor MN58b in human carcinoma models. *Cancer Res* **66**, 427–434.

[38] Beloueche-Babari M, Jackson LE, Al-Saffar NMS, Workman P, Leach MO, and Ronen SM (2005). Magnetic resonance spectroscopy monitoring of mitogen-activated protein kinase signaling inhibition. *Cancer Res* **65**, 3356–3363.

[39] Glunde K and Serkova NJ (2006). Therapeutic targets and biomarkers identified in cancer choline phospholipid metabolism. *Pharmacogenomics* **7**, 1109–1123.

[40] Munster PN, Troso-Sandoval T, Rosen N, Rifkind R, Marks PA, and Richon VM (2001). The histone deacetylase inhibitor suberoylanilide hydroxamic acid induces differentiation of human breast cancer cells. *Cancer Res* **61**, 8492–8497.

[41] Skehan P, Storeng R, Scudiero D, Monks A, McMahon J, Vistica D, Warren JT, Bokesch H, Kenney S, and Boyd MR (1990). New colorimetric cytotoxicity assay for anticancer-drug screening. *J Natl Cancer Inst* **82**, 1107–1112.

[42] Workman P, Twentyman P, Balkwill F, Balmain A, Chaplin D, Double J, Embleton J, Newell D, Raymond R, Stables J, et al. (1998). United Kingdom Co-ordinating Committee on Cancer Research (UKCCCR) Guidelines for the Welfare of Animals in Experimental Neoplasia (Second Edition). *Br J Cancer* **77**, 1–10.

[43] Tyagi RK, Azrad A, Degani H, and Salomon Y (1996). Simultaneous extraction of cellular lipids and water-soluble metabolites: evaluation by NMR spectroscopy. *Magn Reson Med* **35**, 194–200.

[44] Ordidge RJ, Connelly A, and Lohman JAB (1986). Image selected *in vivo* spectroscopy (ISIS). A new technique for spatially selective NMR spectroscopy. *J Magn Reson* **66**, 283–294.

[45] Van der Veen JWC, De Beer R, Luyten PR, and Van Ormondt D (1989). Accurate quantification of *in vivo* ^{31}P NMR signals using the variable projection method and prior knowledge. *Magn Reson Med* **6**, 92–98.

[46] Bergmeyer HU (1974). *Methods of Enzymatic Analysis.* Weinheim, Germany: Verlag Chemie.

[47] Sitter B, Sonnewald U, Spraul M, Fjosne HE, and Gribbestad IS (2000). High-resolution magic angle spinning MRS of breast cancer tissue. *NMR Biomed* **15**, 327–337.

[48] Sankaranarayanapillai M, Tong WP, Maxwell DA, Pal A, Pang J, Bornmann WG, Gelovani JG, and Ronen SM (2006). Detection of histone deacetylase inhibition by noninvasive magnetic resonance spectroscopy. *Mol Cancer Ther* **5**, 1325–1334.

[49] Clark PA, Hostein I, Banerji U, Stefano FD, Maloney A, Walton M, Judson I, and Workman P (2000). Gene expression profiling of human colon cancer cells following inhibition of signal transduction by 17-allyamino,17-demethoxygeldanamycin, an inhibitor of the Hsp90 molecular chaperone. *Oncogene* **19**, 4125–4133.

[50] Negendank WG (1992). Studies of human tumors by MRS: a review. *NMR Biomed* **5**, 303–324.

[51] Moreno A, Lopez LA, Fabra A, and Arus C (1998). ^{1}H MRS markers of tumor growth in intrasplenic tumors and liver metastasis induced by injection of HT-29 cells in nude mice spleen. *NMR Biomed* **11**, 93–106.

[52] Negendank WG, Padavic-Shaller KA, Li C-W, Murphy-Boesch J, Stoyanova R, Krigel RL, Schilder RJ, Smith MR, and Brown TR (1995). Metabolic characterisation of non–Hodgkin's lymphomas *in vivo* with the use of proton-decoupled phosphorus magnetic resonance spectroscopy. *Cancer Res* **55**, 3286–3294.

[53] Milkevitch M, Shim H, Pilatus U, Pickup S, Wehrle JP, Samid D, Poptani H, Glickson JD, and Delikatny EJ (2005). Increases in NMR-visible lipid and glycerol-phosphocholine during phenylbutyrate-induced apoptosis in human prostate cancer cells. *Biochim Biophys Acta* **1734**, 1–12.

[54] MacPhail LB, Chung Y-L, Madhu B, Clark S, Griffiths SR, Kelland LR, and Robinson SP (2005). An investigation of tumor dose response to the vascular disrupting agent 5,6-dimethylxanthenone-4-acetic acid (DMXAA), using *in vivo* magnetic resonance spectroscopy. *Clin Cancer Res* **11**, 3705–3713.

[55] Madhu B, Waterton JC, Griffiths JR, Ryan AJ, and Robinson SP (2006). The response of RIF-1 fibrosarcomas to the vascular-disrupting agent ZD6126 assessed by *in vivo* and *ex vivo* ^{1}H magnetic resonance spectroscopy. *Neoplasia* **8**, 560–567.

[56] Weinberg RA (2007). *The Biology of Cancer.* New York, Garland, 580.

[57] Vaupel P, Kallinowski F, and Okunieff P (1989). Blood flow, oxygen and nutrient supply and metabolic microenvironment of human tumors: review. *Cancer Res* **49**, 6449–6465.

[58] Jain RK and Carmeliet PF (2001). Vessels of death or life. *Sci Am* **285**, 38–45.